

Real-space scaling methods applied to the one-dimensional extended Hubbard model.

I. The real-space renormalization-group method

B. Fourcade and G. Spronken

Département de Génie Physique, Ecole Polytechnique, Montréal, Québec, Canada, H3C 3A7

(Received 14 July 1983; revised manuscript received 12 January 1984)

The real-space renormalization-group method is applied to the one-dimensional extended Hubbard model. It is shown that in the half-filled-band case, the phase diagram consists of two phases and that the transition from the spin-ordered phase to the charge-ordered phase is continuous, a result which differs from that obtained previously from the broken-symmetry Hartree-Fock approximation.

I. INTRODUCTION

The one-dimensional (1D) extended Hubbard Hamiltonian is given by the following expression:

$$H = t \sum_{i\sigma} (c_{i\sigma}^\dagger c_{i+1\sigma} + \text{c.c.}) + U \sum_i n_{i\uparrow} n_{i\downarrow} + G \sum_i n_i n_{i+1} - \mu \sum_i n_i. \quad (1)$$

The first term in (1) is the nearest-neighbor hopping term characterized by the overlap integral t , $2t$ being the half-width of the conduction band. The next two contributions account, respectively, for the intrasite (U) and intersite (G) electron-electron interaction energy. In the last term, μ stands for the chemical potential. The operators $c_{i\sigma}^\dagger$ and $c_{i\sigma}$ are the usual creation and annihilation operators for an electron of spin σ in a Wannier state at site i . The occupation number is defined as $n_{i\sigma} = c_{i\sigma}^\dagger c_{i\sigma}$ and $n_i = n_{i\uparrow} + n_{i\downarrow}$.

In the atomic limit ($t=0$), Bari¹ has shown that in the half-filled-band regime at zero temperature, the system undergoes a first-order phase transition from a charge-ordered state to a Mott state when $U=2G$. Both phases are insulating, and the ground state has either singly occupied sites for $U > 2G$ or alternate empty and doubly occupied sites for $U < 2G$. In the strong attractive intrasite limit ($|U| \gg t, G$) these two states are well separated. Neglecting the states with singly occupied sites, Efetov and Larkin² have shown that (1) is equivalent, for the special case $|U|G = t^2$, to an exactly soluble, free-boson Hamiltonian, a result that was extended to all G by Fowler,³ who has shown that in this strong on-site limit the ground state of the electron gas is a charge-ordered state for all $G > 0$. There are two additional cases for which the Hamiltonian (1) can be exactly solved. On one hand, when $G=0$, (1) reduces to the bare Hubbard model whose exact solution has been obtained by Lieb and Wu.⁴ It has been shown that in the half-filled-band regime, the antiferromagnetic ground state for $U > 0$ becomes the charge-ordered state for $U < 0$.⁵ On the other hand, in the saturated regime (all spins aligned along the same direction), both the intrasite and the intersite interactions between electrons of opposite spins have vanishing matrix elements, and (1) reduces to an equivalent spinless in-

teracting fermion system which can be transformed, using the Wigner-Jordan transformation, into the Heisenberg-Ising linear chain, a well-known system.⁶⁻¹¹ It turns out that in the corresponding half-filled-band case (the number of spinless fermions is half the number of sites) the system undergoes an order-disorder transition when $G/2|t|=1$. For $G/2|t| < 1$, the system is found in a metallic phase, and for $G/2|t| > 1$ it is an insulator having alternate occupied and empty sites. Except for this last case, there is no exact result in the general case for which t , G , and U take arbitrary values, and the properties of (1) can be obtained by means of approximate calculations only. The simplest approach is the broken-symmetry Hartree-Fock approximation which has been performed on (1) by several authors.¹²⁻¹⁵ It was found¹⁴ that the $U/t - G/t$ phase diagram has two phases separated by the transition line $U=2G$. These phases are the antiferromagnetic ordered phase ($U > 2G$) and the charge-ordered phase ($U < 2G$), and the transition across the boundary line $U=2G$ is a first-order transition.

In this, the first of two papers, we investigate some of the properties of the Hamiltonian (1) using the real-space renormalization-group method. This method has been previously applied to many systems, and in particular to two exactly soluble interacting fermion systems: the 1D Hubbard model^{16,17} and the fermion analog of the Heisenberg-Ising linear chain.¹⁸ Aside from the essential singularity at the unstable fixed points of these models, which is recovered but with the wrong critical exponent, it turns out that this method yields results in generally good agreement with the exact results. The ground-state energy is well reproduced and the magnitude of the local moment, for the 1D Hubbard model, is reproduced with great accuracy. This latter result clearly indicates that the real-space renormalization-group method gives reliable information about the nature of the transition. It will be shown that the local moment, for the extended Hubbard model (1), varies continuously as a function of both U and G , and consequently, the charge-ordered-spin-ordered transition is of second order, a result that differs from the previous Hartree-Fock calculation.¹⁴ As we shall show in the following paper,¹⁹ the same result is obtained within the framework of another approximation scheme, the

finite-cell—scaling method.

In the following section we review the method, and proceed to its application to the Hamiltonian (1). The results for the range $G > 0$ and $U \geq 0$ are presented in Sec. III for the half-filled-band case.

II. METHOD

The real-space renormalization-group method essentially consists of dividing the original chain into blocks of finite size. Each block is then solved exactly and the block Hamiltonian, as well as the interblock Hamiltonian,

are projected onto a reduced basis of states of the Hilbert space. Here, the basis is chosen such that the form of the Hamiltonian is preserved through this process. There result new values for the parameters, and the procedure is repeated until one reaches a fixed point.

The method can be made more transparent if the original Hamiltonian (1) is split into its block and interblock parts. Written under the electron-hole—symmetry form, one obtains

$$H^{(n)} = \sum_j H_j^{(n)} + \sum_j H_{j,j+1}^{(n)}, \quad (2)$$

where j is a block index, and

$$H_j^{(n)} = t^{(n)} \sum_{p=1}^{n_s-1} \sum_{\sigma} (c_{j,p\sigma}^\dagger c_{j,p+1\sigma} + \text{c.c.}) + U^{(n)} \sum_{p=1}^{n_s} (\frac{1}{2} - n_{j,p\uparrow})(\frac{1}{2} - n_{j,p\downarrow}) + G^{(n)} \sum_{p=1}^{n_s-1} (1 - n_{j,p})(1 - n_{j,p+1}) + D^{(n)} \sum_{p=1}^{n_s} \hat{1}_{j,p}, \quad (3a)$$

$$H_{j,j+1}^{(n)} = t^{(n)} \sum_{\sigma} (c_{j,n_s\sigma}^\dagger c_{j+1,1\sigma} + \text{c.c.}) + G^{(n)} (1 - n_{j,n_s})(1 - n_{j+1,1}). \quad (3b)$$

Here n is an iteration index and n_s is the number of sites of each block. In (3a) we have made use of the electron-hole symmetry to fix the chemical potential: $\mu = \frac{1}{2}U + 2G$ and $D^{(n)}$ is an additional constant that accounts for the renormalization of the vacuum energy. In (3a), $\hat{1}$ is the identity operator. At the initial step ($n=0$), the Hamiltonian (2) is identical to (1) provided that $t^{(0)}=t$, $G^{(0)}=G$, $U^{(0)}=U$, and $D^{(0)}=-\frac{1}{2}\mu$.

Each block Hamiltonian $H_j^{(n)}$ is solved exactly. There are four quantities which are left invariant by $H_j^{(n)}$: the number of electrons N , the total spin and its projection along a given axis, \tilde{S} and S_z , and the parity Π . Accordingly, the Hilbert space Γ is split into subspaces spanned by the set of kets $\{|N, S, S_z, \Pi, k\rangle\}$ [$\tilde{S}^2 = S(S+1)$], where k is an additional index that identifies a specific ket within a given subspace, the number of these k 's being the dimension of this subspace.

The absolute ground-state energy has been proved by Lieb and Mattis²⁰ to lie within the $S = |S_z|$ subspace where, for a given N , $|S_z|$ takes the lowest possible value. Let us call by $|N, S_z\rangle$ the lowest-energy eigenstate of each $S = |S_z|$ subspace, and by E_N the corresponding eigenenergy. The set $\{|N, S_z\rangle\}$ provides the reduced basis onto which the block Hamiltonian as well as any relevant operator are projected. Of course, this choice of basis is not unique. However, one expects¹⁶ the ground-state properties of the system to be reproduced if the projection is performed onto the basis of the lowest-energy eigenstates.

The set $\{|N, S_z\rangle\}$ spans the subspace $\tilde{\Gamma}$ of Γ . However, this set does not satisfy any closure relation, and the projection onto $\tilde{\Gamma}$ of a given operator, for instance, A_Γ , cannot be used as the definition of the renormalization of this operator. In order to avoid this difficulty, one introduces a new Hilbert space γ spanned by a set of kets, $\{|N', S'_z\rangle\}$, which is related to the former set, $\{|N, S_z\rangle\}$, through a one-to-one mapping; that is to say, to each ket $|N, S_z\rangle$ belonging to $\tilde{\Gamma}$, there is one and only one ket

$|N', S'_z\rangle$ belonging to γ . We require that this new set obey the following closure relation:

$$\sum_{\gamma} |N', S'_z\rangle \langle N', S'_z| = \hat{1}. \quad (4)$$

As a consequence of the one-to-one mapping $\tilde{\Gamma} \leftrightarrow \gamma$, the direct product spaces $\tilde{\Gamma} \otimes \tilde{\Gamma}$ and $\gamma \otimes \gamma$ are identical. Accordingly, for any operator A_Γ defined in Γ , there exists a unique operator A_γ defined in γ such that $\langle i | A_\Gamma | j \rangle = \langle i | A_\gamma | j \rangle$, where $|i\rangle, |j\rangle \in \tilde{\Gamma}$, $|i\rangle, |j\rangle \in \gamma$, and $|i\rangle \leftrightarrow |i\rangle$, $|j\rangle \leftrightarrow |j\rangle$. As a result, both operators A_Γ and A_γ are related through

$$A_\gamma = \sum_{i,j} |i\rangle \langle i | A_\Gamma | j \rangle \langle j |, \quad (5)$$

which defines the renormalization of A_Γ . The isomorphic mapping makes it possible to relate average values of any operator taken in two different renormalization steps. In other words, it gives a meaning to the iterative renormalization process.

The Hilbert space associated with any given site of the original chain is spanned by four vectors: $|0\rangle$, $|1, +\rangle = c_1^\dagger |0\rangle$, $|1, -\rangle = c_1^\dagger |0\rangle$, and $|2, 0\rangle = c_1^\dagger c_1^\dagger |0\rangle$. For the form of the Hamiltonian to be preserved through any renormalization step, the Hilbert space associated with any site of the renormalized chain, which replaces a block of n_s sites of the previous chain, should be spanned by four independent vectors also. Accordingly, at each step, the selected subspace $\tilde{\Gamma}$ of the block Hilbert space Γ is spanned by four vectors of the form $|m, 0\rangle$, $|m+1, +\rangle$, $|m+1, -\rangle$, and $|m+2, 0\rangle$, where m is defined below, and the corresponding Hilbert space γ is spanned by four vectors of the form $|0\rangle$, $|1, +\rangle = c_1^\dagger |0\rangle$, $|1, -\rangle = c_1^\dagger |0\rangle$, and $|2, 0\rangle = c_1^\dagger c_1^\dagger |0\rangle$. It can be shown, with the help of (5), that an iterative construction of the average value of the density operator $d = \langle \rho \rangle = (1/n_s) \sum_i \langle n_i \rangle$ leads to the following relation between the electronic density produced after $n \rightarrow \infty$ steps and the

minimum filling of the block m at each step:

$$d^{(\infty)} = m / (n_s - 1). \quad (6)$$

For the half-filled-band case, $d^{(\infty)} = 1$, and, since m is an

$$H_j^{(n+1)} = |0\rangle\langle 2,0| H_j^{(n)} |2,0\rangle\langle 0| + |1,+ \rangle\langle 3,+ | H_j^{(n)} |3,+ \rangle\langle 1,+ | \\ + |1,- \rangle\langle 3,- | H_j^{(n)} |3,- \rangle\langle 1,- | + |2,0\rangle\langle 4,0| H_j^{(n)} |4,0\rangle\langle 2,0|, \quad (7)$$

which reduces, using the symmetry properties of $H_j^{(n)}$ and the notation introduced above for the eigenvalues of the block Hamiltonian (cf. Appendix), to

$$H_j^{(n+1)} = 2(E_2 - E_3) \left(\frac{1}{2} - n_{j1} \right) \left(\frac{1}{2} - n_{j1} \right) \\ + [3D^{(n)} + \frac{1}{2}(E_2 + E_3)] \hat{1}_j, \quad (8)$$

where the block index j at the step n becomes a site index at the step $n + 1$. Accordingly, one obtains

$$U^{(n+1)} = 2(E_2 - E_3), \quad (9a)$$

$$D^{(n+1)} = 3D^{(n)} + \frac{1}{2}(E_2 + E_3), \quad (9b)$$

where the last term of (9b) accounts for the renormalization of the vacuum energy.

The renormalization of the interblock Hamiltonian is performed similarly. However, this should be performed carefully since the interblock Hamiltonian results from a product of operators defined in different Hilbert spaces, for instance, Γ_j and Γ_{j+1} , and the projection must be done onto the antisymmetric tensor product of the corresponding selected subspaces $\tilde{\Gamma}_j$ and $\tilde{\Gamma}_{j+1}$. The renormalization is then defined with respect to the antisymmetric tensor product of γ_j and γ_{j+1} . Within each Hilbert space, γ_j and γ_{j+1} , the vacuum state is defined up to an arbitrary phase factor which is fixed by the requirement that the form of the hopping term should be preserved through the renormalization process. This leads to the following expression:

$$H_{j,j+1}^{(n+1)} = t^{(n+1)} (c_{j\sigma}^\dagger c_{j+1\sigma} + c.c.) \\ + G^{(n+1)} (1 - n_j)(1 - n_{j+1}), \quad (10)$$

where

$$t^{(n+1)} = t^{(n)} (\langle 2,0 | c_{j,1} | 3,+ \rangle)^2, \quad (11a)$$

$$G^{(n+1)} = G^{(n)} (1 - \langle 2,0 | n_{j,1} | 2,0 \rangle)^2, \quad (11b)$$

for all j (see the Appendix). The results (8) and (10) together with (9), upon summation over the new site index j , yield the renormalized Hamiltonian $H^{(n+1)}$. Equations (9) and (11) are the basic recursion relations for the parameters.

Straightforward calculations show that in the atomic limit ($t=0$), these recursion relations reduce to

$$U^{(n+1)} = U^{(n)}, \quad G^{(n+1)} = \frac{1}{9} G^{(n)}, \quad (12a)$$

for $U > 2G$,

$$U^{(n+1)} = 3U^{(n)} - 4G^{(n)}, \quad G^{(n+1)} = G^{(n)}, \quad (12b)$$

integer, n_s should be an odd number. In the present paper, we shall restrict ourselves to $n_s = 3$, and thus $m = 2$. Accordingly, the renormalized block Hamiltonian $H_j^{(n+1)}$ reads [cf. (5)]

for $G < U < 2G$, and

$$U^{(n+1)} = U^{(n)} - 2G^{(n)}, \quad G^{(n+1)} = G^{(n)} \quad (12c)$$

for $U < G$. For the last two ranges, $U^{(n+1)} < U^{(n)}$. The results obtained from the application of the real-space renormalization-group method to the extended Hubbard Hamiltonian are presented in the following section for both the $t=0$ and $t \neq 0$ cases.

III. RESULTS

The G - U phase diagram ($G > 0, U \geq 0$) for the special case $t=0$ is shown in Fig. 1. According to the recursion relation (12a), starting from any point (U, G) such that $U > 2G$ leads to $U^{(\infty)} = U$ and $G^{(\infty)} = 0$. For this range, the intrasite Hubbard interaction dominates, and the ground-state is a spin-ordered state. For $U < 2G$ [cf. (12b) and (12c)], one finds $U^{(\infty)} \rightarrow -\infty$ and $G^{(\infty)} = G$; both the intrasite and the intersite interactions have identical effects on the electron gas, and the ground state has alternate doubly occupied and empty sites. As a consequence, the phase diagram consists of two phases separated by the boundary line $U = 2G$, in agreement with the exact solution.¹

For $t \neq 0$ the phase diagram shows similar features (Fig. 2), except that the transition line departs significantly

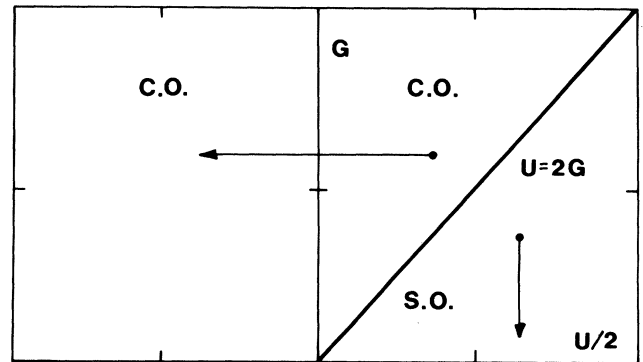


FIG. 1. G - U phase diagram in the atomic limit. The charge-ordered phase (C.O.) and the spin-ordered phase (S.O.) are separated by the boundary line $U = 2G$. The arrows show schematically the different paths followed by the parameters upon renormalization.

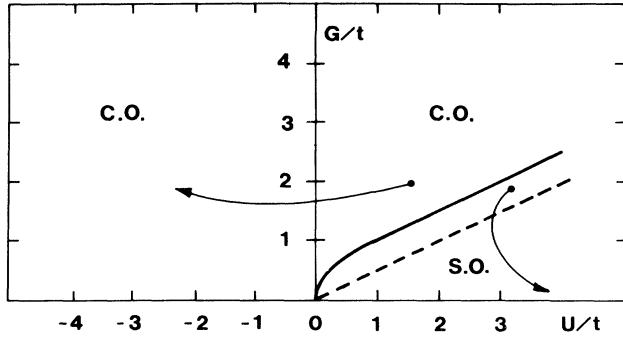


FIG. 2. $G/t-U/t$ phase diagram for $t \neq 0$. The critical line separating the two phases departs significantly from the line $U/t=2(G/t)$ (dashed line). The arrows show the different renormalization paths schematically.

from the line $U=2G$. In Fig. 3 we have plotted $G^{(\infty)}$ as a function of G for both positive and negative values of U , and in Fig. 4 we have plotted $U^{(\infty)}$ as a function of U for several values of G . In both cases, t has been fixed at 1 for simplicity. In all cases, one finds that $t^{(\infty)} \rightarrow 0$. Starting from any point (U, G) above the boundary of Fig. 2 leads to $U^{(\infty)} \rightarrow -\infty$ and $G^{(\infty)} \neq 0$, while starting from a point below the boundary yields $U^{(\infty)} \neq 0$ and $G^{(\infty)} = 0$. For the range $U > 0$, Fig. 3 shows that there is a value for G , say G^* , above which $G^{(\infty)}$ takes finite values. The jump in $G^{(\infty)}$ at G^* becomes more important as U increases [on the scale of Fig. 3(b), this jump is very small]. In Fig. 3(c) we have plotted $G^{(\infty)}$ as a function of G in the vicinity of G^* for large values of U . The results show a discontinuity at $G=G^*$. For each value of U , the set of points (U, G^*) defines the boundary shown in Fig. 2. To the jump in $G^{(\infty)}$ there corresponds a jump in $U^{(\infty)}$. It turns out that $U^{(\infty)}$ (equal to $U^{(\infty)}$ for $G=G^*-0$) and $G^{(\infty)}$ (equal to $G^{(\infty)}$ for $G=G^++0$) are related through $U^{(\infty)} = 2G^{(\infty)}$, and the linear relationship $U=2G$ of the exact solution ($t=0$) becomes, here, $U^{(\infty)} = 2G^{(\infty)}$ ($t^{(\infty)}=0$). In Fig. 5 we have plotted the quantities $U^{(\infty)}$ for $G < G^*$, and $2G^{(\infty)}$ for $G > G^*$, for several values of U in the vicinity of the boundary.

Straightforward calculations show that for a finite open chain with an odd number of sites, the gap in the single-particle excitation spectrum is $\Delta=U^{(\infty)}$ for the spin-ordered regime ($U^{(\infty)} \neq 0, G^{(\infty)} = 0$) and $2G^{(\infty)} - U^{(\infty)}$ for the charge-ordered one ($U^{(\infty)} \rightarrow -\infty, G^{(\infty)} \neq 0$). In the latter case, one can show that the gap in the pair-excitation spectrum is $\Delta=2G^{(\infty)}$. Since $U^{(\infty)} \rightarrow -\infty$, the latter excitation dominates. Hence, the results depicted in Fig. 5 show the gap on an extended scale near the transition. The gap is plotted in Fig. 6 for a wider range of G for both negative and positive values of U . Several conclusions can be drawn from the results of Figs. 3–6: For the range $U > 0$ and $G > 0$, (1) the variation of the gap is continuous at the transition, while (2) its derivative is not, (3) it never vanishes across the boundary, and (4) the nature of the elementary excitations changes from a single-particle-excitation regime (for $U^{(\infty)} \neq 0, G^{(\infty)} = 0$) to one

of pair excitations (for $U^{(\infty)} \rightarrow -\infty, G^{(\infty)} \neq 0$). For the range $U \leq 0, G \geq 0$, the gap vanishes along the semi-infinite ($U \leq 0, G = 0$) line only. For this part of the phase diagram, the elementary excitations are pair excitations.

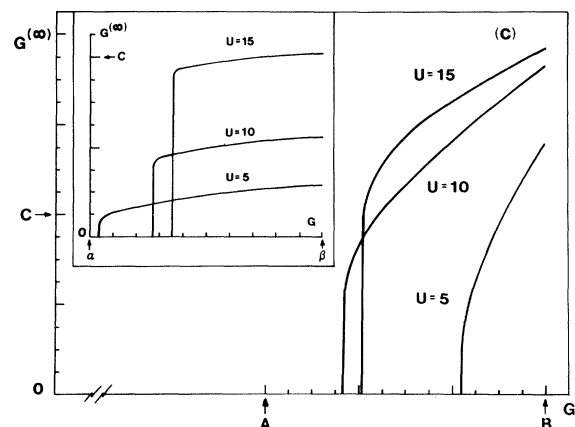
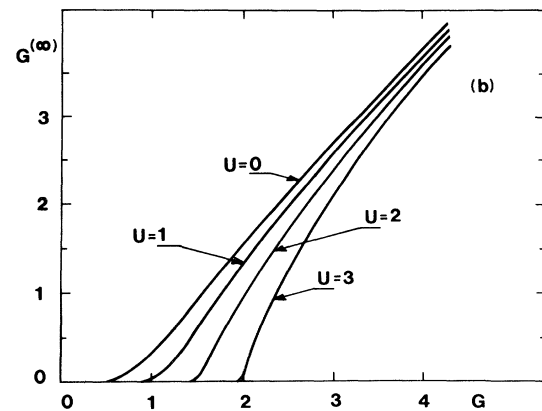
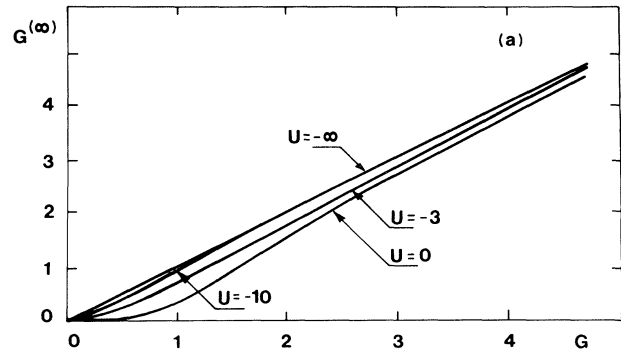


FIG. 3. $G^{(\infty)}$ as a function of G for (a) $U < 0$ and (b) and (c) $U > 0$. In (c), the values of A and B are $U=5-A=1, B=4$; $U=10-A=5, B=8$; $U=15-A=16, B=19$. In the inset, $G^{(\infty)}$ as a function of G is shown on an extended scale near the transition. The values of α and β are, respectively, $\alpha=3.1, \beta=3.125$ for $U=5$, $\alpha=5.825, \beta=5.85$ for $U=10$, and $\alpha=8.5185, \beta=8.531$ for $U=15$. The value of C is $C=2$ for $U=5$ and $C=4$ for $U=10$ and 15 .

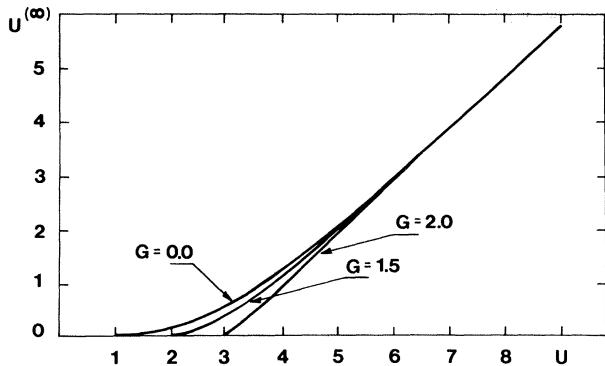


FIG. 4. $U^{(\infty)}$ as a function of U for several values of G .

Our results also indicate that the origin of the G - U plane is an essential singularity. In the case $G=0$ (i.e., the pure Hubbard model), the method yields, in the vicinity of $U=0$, $(U/t)'=(U/t)$, in agreement with the scaling hypothesis.²¹ However, Dasgupta *et al.*¹⁷ have shown that even in the large-cell limit, the results obtained differ from the exact solution, and the singularity is recovered poorly. Along the line $G \geq 0$ ($U=0$), first-order expansion, near $G=0$, yields $(G/t)'=\frac{1}{2}(G/t)$, a result that violates the scaling hypothesis.²² In view of this, we do not expect the real-space renormalization-group method to give reliable results (for the critical exponent that characterizes the opening of the gap, for instance) in the vicinity of $U=G=0$. Accordingly, we did not attempt to perform any calculation around the origin of the G - U plane.

The ground-state energy obtained from¹⁶

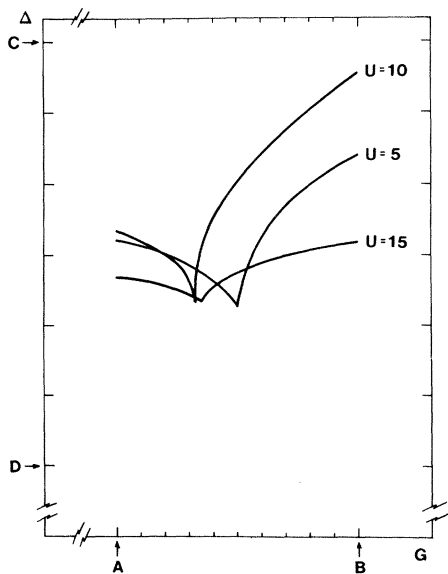


FIG. 5. Plot of the quantity $\Delta=U^{(\infty)}$ below the boundary and $\Delta=2G^{(\infty)}$ above it as a function of G on an extended scale near the boundary. The values of A , B , C , and D are, respectively, $A=3.1$, $B=3.1025$, $C=0.7$, and $D=0.1$ for $U=5$; $A=5.75$, $B=6.0$, $C=7.0$, and $D=1.0$ for $U=10$; and $A=8.5185$, $B=8.531$, $C=11.0$ and $D=5.0$ for $U=15$.

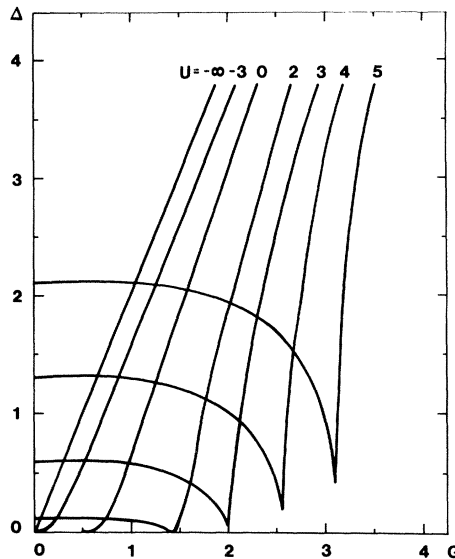


FIG. 6. Gap Δ as a function of G for several values of U .

$$E_g = \lim_{n \rightarrow \infty} \frac{D^{(n)}}{3^n} \tag{13}$$

is plotted in Fig. 7 as a function of U for several values of G . For all G the slope of these curves decreases as U increases, which indicates that the average value of the intrasite interaction energy in (1) vanishes in the large- U limit. Accordingly, there is no doubly occupied site and the system is found in a spin-ordered ground state. This can be best seen in Fig. 8 where we have plotted the average value of $(1/N) \sum_i n_{i\uparrow} n_{i\downarrow}$ as a function of U and G . The local moment M , defined as¹⁶

$$M = \frac{3}{4} \langle (n_{2\uparrow} - n_{2\downarrow})^2 \rangle, \tag{14}$$

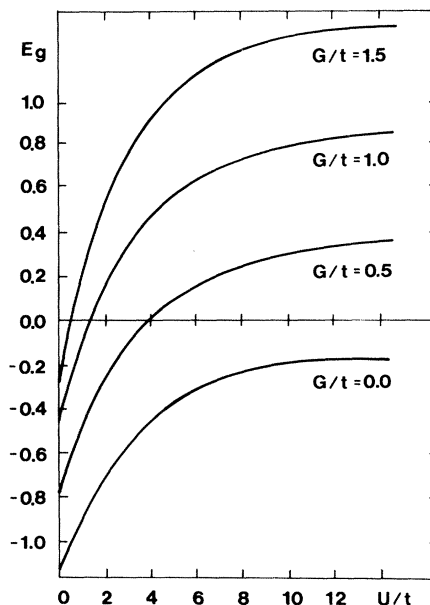


FIG. 7. Ground-state energy E_g as a function of U/t for several values of G/t .

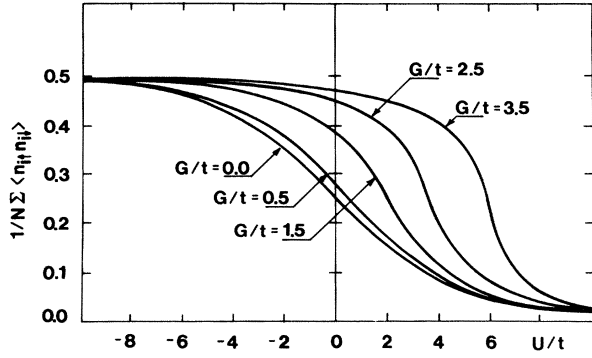


FIG. 8. Average value of $(1/N) \sum_i n_{i\uparrow} n_{i\downarrow}$ as a function of U/t for several values of G/t .

has been iteratively constructed using (5). The result is shown in Fig. 9. M varies continuously across the boundary, and the system undergoes a second-order transition from a charge-ordered phase ($M=0$) through a spin-ordered phase ($M = \frac{3}{4}$). In the vicinity of the boundary, Fig. 9 indicates that the system is found in a mixed spin-ordered—charge-ordered phase.

IV. CONCLUSION

It has been shown that the application of the real-space renormalization-group method to the 1D extended Hubbard model, in the half-filled-band regime, yields results similar to those previously obtained by means of the broken-symmetry Hartree-Fock approximation. There are, however, two main differences: (1) The spin-ordered and charge-ordered phases are separated by a boundary line which reduces to a straight line ($U=2G$) in the atomic limit only, and (2) the transition across the boundary is a continuous phase transition. As a consequence of the latter point, the system, in the vicinity of the transition line, is found in a mixed spin-ordered—charge-ordered phase. As we shall see in the following paper, the results obtained using the finite-cell—scaling method support these conclusions.

ACKNOWLEDGMENTS

We are grateful to S. Sarker and A. Yelon for helpful discussions and suggestions. One of us (B.F.) acknowledges the France-Quebec organization for financial

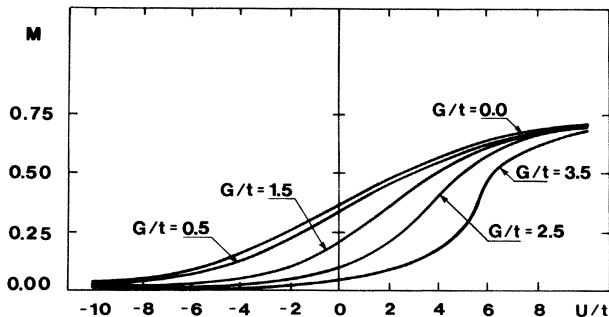


FIG. 9. Magnitude of the local moment M as a function of U/t for several values of G/t .

support. This work was supported in part by the Natural Sciences and Engineering Research Council of Canada.

APPENDIX: UNITARY TRANSFORMATIONS AND PROJECTORS

Within each Γ Hilbert space, the selected basis consists of four states: the nonmagnetic states $|2,0\rangle$ and $|4,0\rangle$, and the magnetic states $|3,+ \rangle$ and $|3,- \rangle$. In both subspaces, the states are related through unitary transformations whose general expressions are²³

$$U_\rho = \exp \left[\sum_i \alpha_i \vec{K}_i \cdot \vec{\rho}_i \right], \quad \alpha_i^2 = -1 \quad (\text{A1})$$

$$U_s = \exp \left[\sum_i \beta_i \vec{Q}_i \cdot \vec{S}_i \right],$$

where $\vec{S}_i = (S_{xi}, S_{yi}, S_{zi})$ and $\vec{\rho}_i = (\rho_{xi}, \rho_{yi}, \rho_{zi})$, with

$$\begin{aligned} S_{xi} &= c_{i\uparrow}^\dagger c_{i\downarrow} + c_{i\downarrow}^\dagger c_{i\uparrow}, \\ S_{yi} &= \rho (c_{i\downarrow}^\dagger c_{i\uparrow} - c_{i\uparrow}^\dagger c_{i\downarrow}), \\ S_{zi} &= n_{i\uparrow} - n_{i\downarrow}, \\ \rho_{xi} &= c_{i\uparrow}^\dagger c_{i\downarrow}^\dagger + c_{i\downarrow} c_{i\uparrow}, \\ \rho_{yi} &= \rho (c_{i\downarrow} c_{i\uparrow} - c_{i\uparrow}^\dagger c_{i\downarrow}^\dagger), \\ \rho_{zi} &= n_{i\uparrow} + n_{i\downarrow} - 1, \end{aligned} \quad (\text{A2})$$

and where \vec{K}_i and \vec{Q}_i are arbitrary unit vectors, and α_i and β_i are the parameters of the transformations. These quantities can be chosen such that

$$U_\rho c_{i\sigma} U_\rho^\dagger = (-1)^i c_{i\bar{\sigma}}^\dagger, \quad U_s c_{i\sigma} U_s^\dagger = c_{i\bar{\sigma}}. \quad (\text{A3})$$

The former accounts for the electron-hole exchange, while the latter amounts to the spin inversion. Both transformations commute with the block Hamiltonian. Accordingly, one obtains:

$$|4,0\rangle = U_\rho |2,0\rangle, \quad |3,+ \rangle = U_s |3,- \rangle, \quad (\text{A4})$$

and the nonmagnetic states, as well as the magnetic ones, are degenerate. The parity operator Π , defined as

$$\Pi c_{i\sigma} \Pi = c_{n_s - i + 1, \sigma}, \quad \Pi^2 = \hat{1} \quad (\text{A5})$$

also commutes with the Hamiltonian. The expressions (A1)–(A5) can be used to relate the different matrix elements of the creation, annihilation, and occupation-number operators involved in the renormalization of both the block and the interblock Hamiltonians.

The projectors involved in (7) can be written in terms of fermion operators,²⁴

$$|0\rangle\langle 0| = (1 - n_\uparrow)(1 - n_\downarrow), \quad |1,+ \rangle\langle 1,+ | = (1 - n_\downarrow)n_\uparrow, \quad (\text{A6})$$

$$|1,- \rangle\langle 1,- | = (1 - n_\uparrow)n_\downarrow, \quad |2,0\rangle\langle 2,0| = n_\uparrow n_\downarrow,$$

from which (8) follows. Similar expressions lead to (10).

- ¹R. A. Bari, Phys. Rev. B **3**, 2662 (1971).
²K. B. Efetov and A. I. Larkin, Zh. Eksp. Teor. Fiz. **69**, 764 (1975) [Sov. Phys.—JETP. **42**, 390 (1976)].
³M. Fowler, Phys. Rev. B **17**, 2989 (1978).
⁴E. Lieb and F. Wu, Phys. Rev. Lett. **20**, 1445 (1968).
⁵H. Shiba, Prog. Theor. Phys. **48**, (6B), 2171 (1972).
⁶R. Orbach, Phys. Rev. **112**, 309 (1958).
⁷C. N. Yang and C. P. Yang, Phys. Rev. **147**, 303 (1966).
⁸C. N. Yang and C. P. Yang, Phys. Rev. **150**, 321 (1966).
⁹C. N. Yang and C. P. Yang, Phys. Rev. **150**, 327 (1966).
¹⁰C. N. Yang and C. P. Yang, Phys. Rev. **151**, 258 (1966).
¹¹J. des Cloizeaux and M. Gaudin, J. Math. Phys. **7**, 1384 (1966).
¹²S. Robaszkiewicz, R. Micnas, and K. A. Chao, Phys. Rev. B **24**, 4018 (1981).
¹³S. Robaszkiewicz, Phys. Status Solidi B **59**, K63 (1973).
¹⁴D. Cabib and E. Callen, Phys. Rev. B **12**, 5249 (1975).
¹⁵A. Madhukar, Solid State Commun. **13**, 1767 (1973).
¹⁶J. E. Hirsch, Phys. Rev. B **22**, 5259 (1980).
¹⁷C. Dasgupta and P. Pfeuty, J. Phys. C **14**, 717 (1981).
¹⁸G. Spronken, R. Jullien, and M. Avignon, Phys. Rev. B **24**, 5356 (1981).
¹⁹B. Fourcade and G. Spronken, following paper, Phys. Rev. B **29**, 5096 (1984).
²⁰E. Lieb and D. Mattis, Phys. Rev. **125**, 164 (1962).
²¹S. Sarker (private communication).
²²V. J. Emery, in *Highly Conducting One-Dimensional Solids*, edited by J. T. Devreese, R. P. Evrard, and V. E. van Doren (Plenum, New York, 1979).
²³C. Castellani, C. Di Castro, D. Feinberg, and J. Ranninger, Phys. Rev. Lett. **43**, 1957 (1979).
²⁴J. Hubbard, Proc. R. Soc. London, Ser. A **277**, 237 (1964).